

Ground state and glass transition of the RNA secondary structure

Sheng Hui and Lei-Han Tang ^a

Department of Physics, Hong Kong Baptist University, Kowloon Tong, Hong Kong SAR, China

November 5, 2018

Abstract. RNA molecules form a sequence-specific self-pairing pattern at low temperatures. We analyze this problem using a random pairing energy model as well as a random sequence model that includes a base stacking energy in favor of helix propagation. The free energy cost for separating a chain into two equal halves offers a quantitative measure of sequence specific pairing. In the low temperature glass phase, this quantity grows quadratically with the logarithm of the chain length, but it switches to a linear behavior of entropic origin in the high temperature molten phase. Transition between the two phases is continuous, with characteristics that resemble those of a disordered elastic manifold in two dimensions. For designed sequences, however, a power-law distribution of pairing energies on a coarse-grained level may be more appropriate. Extreme value statistics arguments then predict a power-law growth of the free energy cost to break a chain, in agreement with numerical simulations. Interestingly, the distribution of pairing distances in the ground state secondary structure follows a remarkable power-law with an exponent $-4/3$, independent of the specific assumptions for the base pairing energies.

PACS. 87.14.Gg DNA, RNA – 87.15.-v Biomolecules: structure and physical properties – 64.70.Pf Glass transitions

1 Introduction

The three-dimensional structure (i.e. conformation) of biomolecules is a fascinating topic due to its fundamental importance in modern biology[1]. Link between the structure of a biopolymer and its sequence information, however, remains at an empirical level due to the hitherto unyielding computational complexity in predicting the shape of a heterogeneous polymer[2,3,4,5,6]. At the heart of the problem is the lack of a general understanding on the energetics of a collapsed polymer in the presence of sequence-specific contact energies. Such a situation has been compared with the low temperature behavior of the spin glass model[7,8], although the chain constraint and the unknown nature of sequence specificity may invalidate the analogy.

In the present paper, we focus on the secondary structure of RNA molecules[9,10,11,12,13]. RNA, like DNA, is a long chain molecule made of four different types of nucleotides: adenine (A), uracil (U), guanine (G) and cytosine (C). Under normal physiological conditions, an RNA molecule folds into a relatively compact shape which can be loosely described as a mixture of double-stranded helical segments (known as stems) and occasional single-stranded bulges and hairpins with tertiary contacts. The helical segments are stabilized by base-pairing and base stacking which represent dominant contributions to the energy of a folded structure. Unlike a ds-DNA molecule, however, each helical segment is made of two complemen-

tary segments from different parts of the same chain, running in opposite directions. The matching of bases to form the Watson-Crick A-U and G-C pairs, and the energetically less favorable wobble G-U pairs defines the secondary structure of an RNA molecule. The problem of RNA secondary structure prediction is then to find the map of optimal pairings for a given sequence of the nucleotides (the primary structure)[14]. At finite temperatures, one has to consider structures that are not necessarily optimal in energy, but are nevertheless important due to their configurational entropy.

Compared to protein folding, RNA secondary structure prediction is a simpler problem due to the saturation of base-pairing[9]. In particular, for RNA molecules without the so called “pseudoknots”, pairing of bases in an RNA molecule may be represented by one-dimensional, non-intersecting rainbow diagrams[15]. Thanks to this topological constraint, the partition function of a chain of N bases can be determined through an exact dynamic programming algorithm whose computational complexity scales as N^3 [16,17]. Consequently, chains of length up to a few thousand bases can be readily investigated numerically.

From a statistical mechanics point of view, the key issues with regard to RNA secondary structures include a classification of possible phases of the chain in the limit $N \rightarrow \infty$, and the characteristics of the equilibrium structures in each of these phases[13,15]. At sufficiently high temperatures, it is generally agreed that the system is in a “molten phase” with non-specific base-pairing. Various statistical properties of this phase, including the distri-

^a e-mail: lhtang@hkbu.edu.hk

bution of pairing distances, are known through the analytic solution to the homopolymer version of the RNA problem[18]. A defining property of the molten phase is the universal amplitude of the logarithmic excess entropy of a finite chain[15]. As the temperature decreases, a new type of behavior, with properties typical of disordered systems, is seen. However, many details remain controversial[19,20,21,22,23].

Several simplifying models have been introduced in the study of the low temperature glass phase of an RNA molecule. Higgs considered a random heteropolymer model of RNA secondary structure formation[19]. In his model, only Watson-Crick pairing is allowed and each such pair is assigned a negative energy. Through numerical simulations of random sequences, he observed that the ground state is highly degenerate and the system at low temperatures exhibits a broad distribution of the overlap function. The same conclusion was reached in a recent work by Pagnani *et al.* who also studied the molten-to-glass transition[20]. The existence of a spin-glass type ground state in such a model is however disputed by Hartmann.[21]

Bundschuh and Hwa have recently carried out extensive analytic and numerical studies of the RNA secondary structure problem[15]. They have discussed in particular the nature and energetics of low-energy excitations in the glass phase, and presented a proof for the existence of a finite-temperature glass transition. They have shown that the scaling of pairing distances in the glass phase follows a different power from that of the molten phase (see discussion in Sec. 3.2). In addition, the finite-size correction to the free energy (termed pinching energy by the authors) grows as a power-law of the chain length, but the exponent is small and nonuniversal.

Krzakala *et al.*[22] introduced an alternative measure of the sequence-specific pairing which is a characteristic of the low temperature glass phase. Their approach is based on an analogy to the directed polymer problem[24] and the replica method. Their conclusion on the existence of a finite-temperature glass transition is in agreement with previous work.

While the quantities introduced by Bundschuh and Hwa, and by Krzakala *et al.* provide effective measures of the glassy order in the low temperature phase, there is yet no microscopic understanding of the origin of the scale-dependent energies as seen in numerical work. In particular, there is no compelling reason why power-law forms are the preferred choice for the observed scale dependence. This question is important not only from a theoretical point of view, but also when considering the effect of sequence mutation and environmental perturbations (such as tertiary contacts, pseudoknots, and magnesium ions, etc.) on the RNA secondary structure. Therefore a better characterization of the properties of the low-temperature phase is desirable.

The paper is organized as follows. In Sec. 2 we introduce the random pairing energy model studied in the present work and briefly review the numerical scheme used for exact computation of ground state and finite temperature properties. Section 3 contains results and analysis of various properties in the ground state. The behavior of

the system at finite temperatures is discussed in Sec. 4. In Sec. 5 we consider other specification of the random pairing energy and their effect on the properties of the ground state. Section 6 presents a summary and our main conclusions.

2 The model and dynamic programming

The statistical mechanics of the secondary structure of random RNAs is reviewed in Ref.[15]. An RNA molecule is defined by its nucleotide sequence. A secondary structure of the molecule is a pairing pattern of bases on the sequence, where each base (indexed by its position i in the sequence) has at most one partner. As in most previous studies, we consider here only secondary structures that obey the “noncrossing” constraint, i.e., if base i pairs with base $j > i$, and another base $k > i$ pairs with base $l > k$, then either $i < j < k < l$ (separated) or $i < k < l < j$ (nesting). This class of structures, which are the most common in nature, form the configuration space of the RNA secondary structures considered below.

Realistic prediction of the thermodynamically favored RNA secondary structures requires a large parameter set derived empirically from pains-taking thermodynamic measurements over the years[25]. Its main purpose is to differentiate accurately local pairing alternatives. This complication, we believe, is not necessary for a statistical characterization of the scaling properties in the low temperature phase and around the glass transition in the random sequence ensemble. Instead, we consider here a much simpler model where the energy of a secondary structure S is given by,

$$E[S] = \sum_{(i,j) \in S} \epsilon_{i,j}, \quad (1)$$

where $\epsilon_{i,j}$ is the pairing energy of base i with base j . The sum is over all base pairings (i, j) of S .

To complete the description of the model, we need to assign values to the pairing energies $\epsilon_{i,j}$ for a given nucleotide sequence. The standard choice is to make $\epsilon_{i,j}$ dependent on the two nucleotides involved. For the random sequence ensemble, an alternative approach is to choose $\epsilon_{i,j}$ as independent random variables, as suggested in Ref.[15]. This was motivated at first by analytical considerations and supported by numerical evidence. In fact, the two approaches become quite identical when the alphabet size exceeds sequence length, as then every possible pair has a different combination of partners for a typical random sequence. Considering that, for real RNA, each helical segment typically contains a consecutive stack of five or more paired bases (with more than $4^5 = 1024$ possible sequences on each side), one may view the second approach as defining a coarse-grained model on the scale of a helical segment. Previous work on sequence alignment has shown that the matching energy of two randomly selected sequences follows a distribution with an exponential tail[26,27,28,29]. Thus, as a coarse-grained model of RNA secondary structures in the sense described above,

we choose $\epsilon_{i,j} < 0$ to be independent random variables satisfying the distribution,

$$P(\epsilon) = \epsilon_0^{-1} \exp(\epsilon/\epsilon_0), \quad (2)$$

where $\epsilon_0 = 1$ sets the only energy scale of the problem.

Due to the noncrossing constraint on the pairing patterns, the partition function

$$Z(N) = \sum_S \exp(-E[S]/T) \quad (3)$$

of an RNA molecule of N bases at temperature T can be calculated using a dynamic programming algorithm[16,17]. This is done based on the recursive relation

$$Z_{i,j} = Z_{i,j-1} + \sum_{k=i}^{j-1} Z_{i,k-1} e^{-\epsilon_{k,j}/T} Z_{k+1,j-1}. \quad (4)$$

Here $Z_{i,j}$ denotes the partition function of a contiguous segment of the molecule from position i to position j . Starting from the shortest segments of one base each with $Z_{i,i} = 1, i = 1, 2, \dots, N$, one obtains the partition function $Z(N) \equiv Z_{1,N}$ in $O(N^3)$ elementary computations. At $T = 0$, the following equation can be used instead to calculate the ground state energies,

$$E_{i,j} = \min_{i \leq k \leq j} \{E_{i,k-1} + E_{k+1,j-1} + \epsilon_{k,j}\}, \quad (5)$$

where as a convention we set $\epsilon_{i,i} = 0$ for all i , and $E_{i,j} = 0$ for $i \geq j$.

3 The ground state

In this section we present numerical results regarding the ground state of an RNA molecule in the random sequence ensemble. Chains up to $N = 2048$ bases are investigated, with a minimum of 1000 realizations of the pairing energies. Results for shorter chains are obtained as a byproduct in the computation.

3.1 Ground state energy

It has been suggested[15,22] that the statistical mechanics of the RNA problem may be closely related to that of a directed polymer in a disordered medium, which has been studied extensively in the past[30]. In the latter case, the ground state energy of the polymer (or its free energy at finite T) contains a finite-size correction which grows as a power of the chain length[31,32]. This energy is of the same order as the disorder-induced energy fluctuations, with an exponent that takes a universal value throughout the low temperature phase. It is thus interesting to examine such corrections for the RNA problem as well.

The origin of an excess energy associated with a chain of finite length can be appreciated with the help of Fig. 1. Dashed lines in the figure indicate pairing of the bases. Cutting the chain in the middle yields two shorter chains

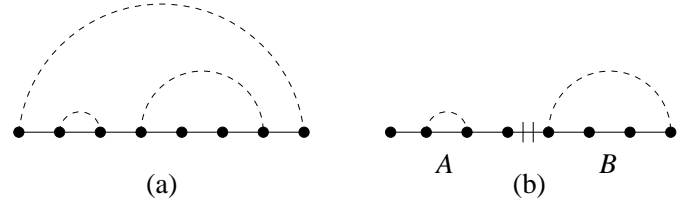


Fig. 1. Rainbow diagrams illustrating allowed base pairing (dashed line) on (a) a single chain, and (b) two separate parts when the chain is broken in the middle.

half of the original size. All pairing patterns of the two shorter chains can be realized on the longer chain, but the reverse is not true. Therefore the free energy of the chain increases when it is broken into smaller parts. This property translates directly to an excess free energy for a chain of finite length.

The importance of quantifying this excess energy has been stressed by Bundschuh and Hwa[15]. Due to the non-crossing constraint, when two bases i and j on the chain form a pair, those within the segment delimited by the two are only allowed to pair among themselves. Therefore any pairing of the bases effectively defines a finite system isolated from the rest of the chain. For the pairing to be energetically favorable, its energy $\epsilon_{i,j}$ must offset the energy cost for splicing out the segment inbetween. Arguments along this line can be used to discuss the stability of a given state as done in Ref. [15] to construct a lower bound on the glass transition temperature.

Here we examine not only the average value but also the distribution of the excess energy as a function of the chain length. Due to the statistical fluctuations in the bond energies, the total ground state energy $E(N)$ of a chain of length N has a fluctuation proportional to $N^{1/2}$. This background fluctuation can be eliminated using the construction shown in Fig. 1(b). A chain of length $2N$ is formed by joining two chains A and B , each of length N . Let $\Delta E_N \equiv E_{1,N} + E_{N+1,2N} - E_{1,2N}$ be the energy gained when bases on chain A are allowed to pair with bases on chain B to form the ground state of the full chain. Apart from the energy of a single pair, this quantity is identical to the pinching energy introduced in Ref.[15]. Chemically, it can be considered as the heat of “reaction” that brings the two halves together. Obviously, ΔE_N is typically positive but may happen to be zero when the ground state of the full chain breaks into two independent halves.

Figure 2(a) shows the normalized distribution $P(\Delta E, N)$ of ΔE_N for $N = 2, 4, 8, \dots, 1024$ on semi-log scale. As N increases, the peak of each curve shifts to the right while at the same time its width also increases. In addition, there is a finite statistical weight $P_0(N) \sim N^{-4/3}$ at $\Delta E = 0$ [see Fig. 4(a)] Figure 2(b) shows a scaling plot of the distributions. Here $\langle \Delta E_N \rangle$ and $W_N = \sqrt{\langle \Delta E_N^2 \rangle - \langle \Delta E_N \rangle^2}$ denote the mean value and standard deviation of ΔE_N , respectively. Convergence to a limiting form at $N = \infty$ starts from the middle of each curve and gradually extends over to the wings. Interestingly, the tail of the distributions at large ΔE decays as a simple exponential.

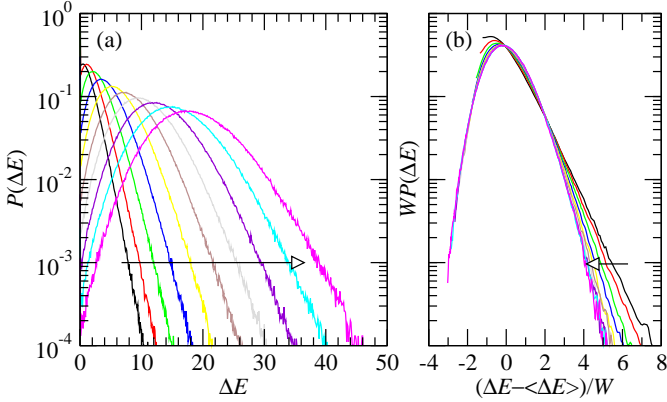


Fig. 2. (a) Distribution of the excess energy ΔE_N of a finite chain for $N = 2, 4, \dots, 1024$. (b) Convergence to a limiting form with zero mean and unit variance. Arrows indicate the direction of increasing N .

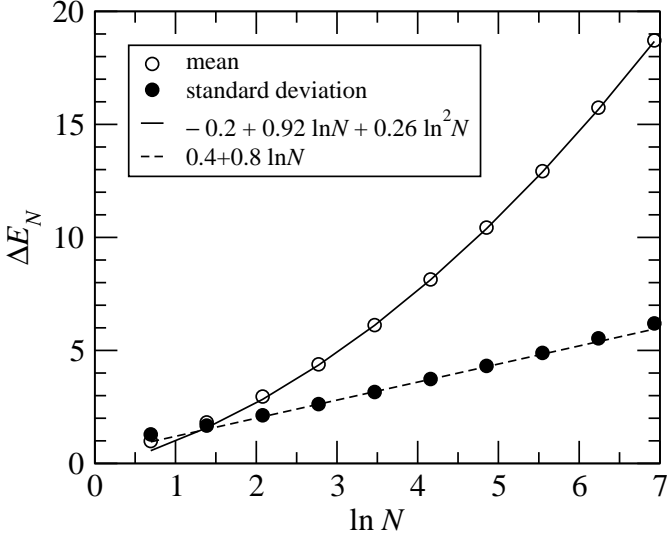


Fig. 3. Mean value and standard deviation of ΔE_N against $\ln N$. Solid and dashed lines represent polynomial fits to the data.

Figure 3 shows $\langle \Delta E_N \rangle$ and W_N against $\ln N$. It is evident that the two quantities are not proportional to each other, i.e., the distributions shown in Fig. 2 can not be collapsed with a single energy scale at each N . Nevertheless, the data can be represented nicely by a quadratic function in $\ln N$ for $\langle \Delta E_N \rangle$, and a linear function in $\ln N$ for W . This suggests that the disorder averaged ground state energy can be written in the form,

$$\langle E(N) \rangle = e_0 N + a + b \ln N + c \ln^2 N, \quad (6)$$

where e_0 is the energy per base in the infinite size limit. From the fit we obtain $a = 0.81$, $b = 1.28$, and $c = 0.26$.

Although the logarithmic form (6) fits the data nearly perfectly, a power-law dependence can not be ruled out based on the numerical data alone.[15,22] Previously, Bundschuh and Hwa[15] made the suggestion that the logarithmic size dependence is more appealing given the small and nonuniversal exponent obtained from various models.

Here we show that the difference in behavior for $\langle \Delta E_N \rangle$ and W_N is still consistent with a single energy scale at each N which grows as $\ln N$. In such a scenario, the $\ln^2 N$ term arises naturally as $\langle \Delta E_N \rangle$ also contains contributions from smaller scales. Specifically, with reference to Fig. 1(b), we may first group bases on either side of the break into zones that are evenly spaced on a logarithmic scale, according to their distance R (measured in terms of number of bases along the chain) to the breaking point. Let $l = \ln R$ be the index of zone l with a width of order R , and suppose that the typical total energy increase of bases in the zone caused by the break is proportional to $\ln R$. Adding up contributions up to $l = \ln N$ yields the desired $\ln^2 N$ dependence. In comparison, fluctuations of ΔE_N do not contain this cumulative effect.

The $\ln N$ energy scale may be motivated from the extreme value statistics argument developed in Refs.[15,26,27,28,29]. According to Eq. (5), when a new base is added to the end of a chain of length N , optimal pairing with interior bases is determined by the competition between the energy cost for perturbing the existing ground state [i.e., the first two terms on the right-hand-side of Eq. (5)], and the energy gain from the newly formed pair. The perturbation is at its weakest when the partner base k is located at either end of the chain. In such a situation, the number of bases at such distances is small, so the available choices for the bond energy $\epsilon_{k,j}$ are rather limited. On the other hand, when k resides in the middle of the chain, the perturbation is the strongest, but then there are of order N choices for $\epsilon_{k,j}$ which, according to the extreme value statistics, yield a typical energy gain proportional to $\ln N$. If ΔE_N grows as a power of N , this energy gain will not be enough to offset the energy cost associated with the perturbation. Consequently pairing with a base in the middle of the chain is extremely unlikely. This however would imply that the chain contains almost exclusively short-distance pairs. If this were the case, the system would have a finite correlation length and a bounded ΔE_N , which contradicts our original assumption. Self-consistency thus requires ΔE_N to grow slower than any power of N , but at least as fast as $\ln N$.

3.2 Pairing statistics

In addition to the ground state energy, we have examined the statistics of pairing distance d in the ground state. When two bases i and $j > i$ form a pair, their pairing distance is defined as $d_{ij} = j - i$. In fact, for a chain of length N , pairs of size d are equivalent to pairs of size $N - d$. This becomes evident if we join the two ends of the chain to form a circle, in which case distance between the two bases is given by the smaller of d and $N - d$. Let $P_s(d)$ be the distribution of d . Symmetry then yields $P_s(d) = P_s(N - d)$. Figure 4(a) shows the distribution $P_s(d)$ for a chain of length $N = 2048$, averaged over 1000 realizations of the $\epsilon_{i,j}$'s. From the plot, we see that, apart from those data points near $d \simeq N/2$ which are influenced by finite-size effects, $P_s(d)$ follows a power-law function d^η with an exponent $\eta = -4/3$. Also shown in the figure is

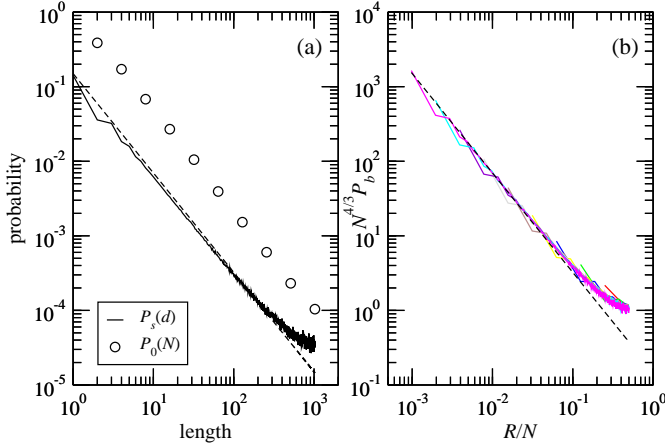


Fig. 4. Pairing statistics in the ground state. (a) Distribution $P_s(d)$ of pairing distance d at $N = 2048$ (solid line). Also shown is $P_0(N)$ against N (circles). (b) A scaling plot of the distribution of the optimal break point for $N = 2, 4, \dots, 1024$. Dashed line in both figures indicates a power-law function with an exponent $\eta = -4/3$.

$P_0(N)$, the probability that the ground state breaks into two independent halves as shown in Fig. 1(b), against N which has a similar behavior. Note that, for each N , $P_0(N)$ is the same as $P(\Delta E)$ at $\Delta E = 0$ [cf. Fig. 2(a)].

We have also examined the statistics of the location of base k where the minimum on the right hand side of Eq. (5) is achieved. Let R be the distance of this base to its partner base j . The distribution $P_b(R, N)$, with N being the length of the interval (i, j) , is shown in Fig. 4(b) using the scaled variables. Here $N = 2, 4, 8, \dots, 1024$. From the data collapse we conclude that $P_b(R, N)$ obeys scaling,

$$P_b(R, N) = N^{-4/3} \Phi(R/N), \quad (7)$$

where $\Phi(x) \sim x^{-4/3}$ for $x \ll 1$.

The scaling properties of base pairing in the ground state as discussed above are consistent with the roughness of “mountain diagrams” introduced in Ref.[15]. In the latter representation, a given secondary structure is mapped to a height profile following a simple rule: starting from one end of the chain, say $i = 0$ with $h_0 = 0$, one proceeds successively to the right, setting $h_i = h_{i-1} + 1$ ($h_i = h_{i-1} - 1$) if base i is paired with base $j > i$ ($j < i$), and $h_i = h_{i-1}$ if base i is unpaired. Bundschuh and Hwa have shown that the average value of h_i as defined above grows as a power-law of the chain length N , $\bar{h} \sim N^\zeta$, where the “roughness exponent” $\zeta = \zeta_g = 0.67 \pm 0.02$, considerably larger than its value $\zeta_0 = 1/2$ in the molten phase. As shown in Ref.[22], the two exponents ζ and η satisfy a general scaling relation,

$$\zeta = 2 + \eta. \quad (8)$$

Equation (8) holds both in the ground state and in the molten phase, where $\eta_0 = -3/2$ has been calculated exactly.

4 Finite temperature properties and the glass transition

At finite temperatures, one needs to consider the entropy associated with alternative pairing to determine the equilibrium structure of an RNA molecule. Comparing Eq. (4) with Eq. (5), we see that qualitatively two types of behavior can be distinguished: (i) only one or a few terms on the right hand side of (4) contribute to $Z_{i,j}$, in which case the situation is similar to that of the ground state; (ii) the number of terms that contribute significantly to $Z_{i,j}$ grows with the chain length, in which case pairing becomes non-specific and one is in the molten phase.

As a quantitative criterion that differentiates the two situations, Bundschuh and Hwa[15] proposed to examine the size dependence of the free energy cost for imposing a pairing (termed “pinching”). At sufficiently high temperatures, the pinching free energy ΔF grows with the pair size N as $\frac{3}{2}T \ln N$, and hence is purely entropic. Based on an estimate of the energy gain for the best matched pair forbidden by the pinch, Bundschuh and Hwa argued that this behavior cannot continue below a certain temperature, and hence a glass transition is expected to take place. Therefore the size-dependence of ΔF can be used to locate the phase transition point.

Following this line of thinking, we consider the statistics of $\Delta F_N \equiv T \ln(Z_{1,2N}/Z_{1,N}Z_{N+1,2N})$ which is the finite temperature analog of ΔE_N defined in the previous section. Figure 5(a) shows the mean value of ΔF_N against $\ln N$, with the high temperature behavior[15] $(3/2)T \ln N$ subtracted from the data. For $T = 1.25$ and below, there is a clear upward curvature in each data set, indicating presence of a $\ln^2 N$ term, though its amplitude decreases with increasing temperature. At $T = 1.5$ and 1.75, however, deviations from the expected high temperature behavior is weak. Figure 5(b) shows the standard deviation $W_{F,N} \equiv \sqrt{\langle \Delta F_N^2 \rangle - \langle \Delta F_N \rangle^2}$ against $\ln N$. Using data points at large N , we extracted the slope $A(T)$ of each curve and plotted the result against T as in the inset. The result can be summarized as,

$$W_{F,N} = \begin{cases} A(T) \ln N + B(T), & T < T_g; \\ B(T), & T > T_g. \end{cases} \quad (9)$$

Here $A(T) = A_0(T - T_g)^2$, with $T_g \simeq 1.7$.

The simple functional forms which fit well the numerical data strongly suggest that there is an underlying simple mathematical structure. It is quite conceivable that a renormalization group theory, similar to the one introduced in Ref. [27] for the unbinding transition of two heteropolymers, can be devised. In the absence of such a theory, Eq. (9) should merely be considered as a convenient representation of numerical data.

5 Other models for the pairing energy

We have argued in Sec. 2 that Eq. (2) provides a generic description of the distribution of pairing energies on a

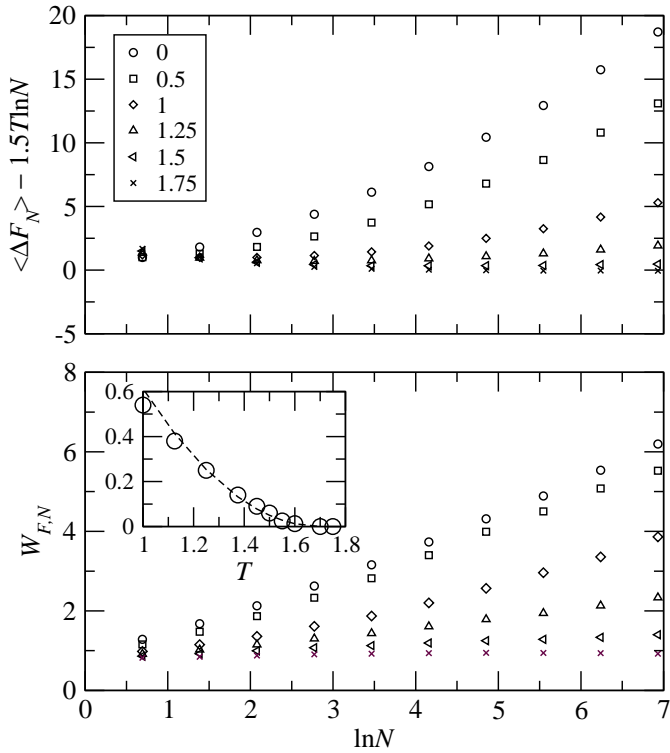


Fig. 5. (a) Mean and (b) standard deviation of ΔF_N against $\ln N$ at a set of temperatures below and above the glass transition. Inset in (b) shows the slope of each curve (and additional ones not shown) against temperature. Dashed line is a quadratic fit with $T_g = 1.7$.

coarse-grained scale. To verify this hypothesis, and to find out to what extent the scaling properties obtained under (2) remain universal, we consider in this section other forms of the pairing energy, and carry out a comparative study of their ground state properties.

5.1 A sequence-based model

To get a flavor of the similarities and differences between random sequence models (with N random variables) and random pairing energy models (with N^2 random variables), we consider here a simplified four-nucleotide model incorporating the essential features of base-pairing energetics. In addition to the Watson-Crick A-U and G-C pairs, we allow the less favorable G-U pair. A stacking energy is included for the propagation of short helices, i.e., if two consecutive bases i and $i + 1$ pair with j and $j - 1$, respectively, an additional energy E_s is gained. The minimal hairpin loop length is set at 4 nt. Results presented below are for the following choice of energy parameters: $E_s = -3$; $E_{GC} = -3 - E_s$; $E_{AU} = -2 - E_s$; $E_{GU} = -1 - E_s$. With this specification, isolated pairings are disfavored. In the ground state, the typical length of a helix is about five base pairs for a random sequence.

Figure 6 shows the mean value and standard deviation of ΔE_N against $\ln N$ for the random sequence ensemble. The behavior is very similar to that of Fig. 3. We have also

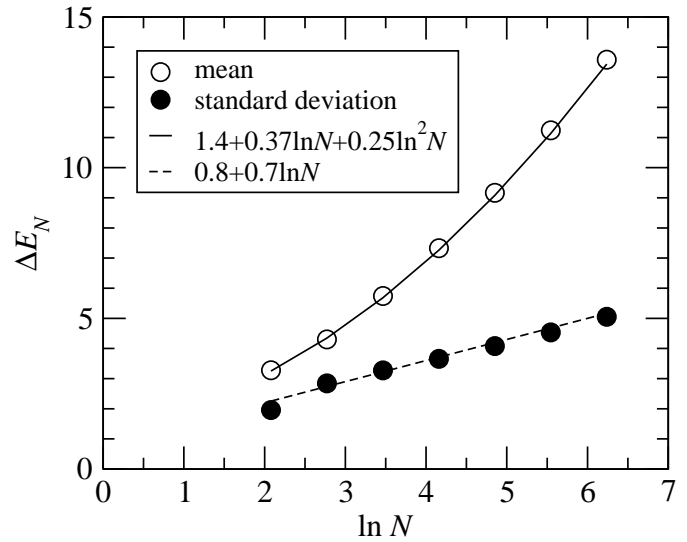


Fig. 6. Mean value and standard deviation of the excess energy of a finite chain in the random sequence ensemble.

examined the statistics of the pairing distances whose distribution fits well to the scaling form (7) with $\eta = -4/3$. These and other properties of the ground state will be reported in detail elsewhere.

5.2 Power-law distribution of the pairing energy

As we mentioned above, the logarithmic size dependence of pairing energies is a generic feature of matching statistics for random sequences. Through evolution, however, sequences that lead to more stable structures may be selected for functional advantages, including possibly RNA's with longer matched segments. Indeed, the secondary structure of many real RNA's show extended stretches of duplicates which are not expected of a random sequence. This observation motivates us to examine the ground state energetics and pairing pattern under a power-law distribution of the pairing energies,

$$P(\epsilon) = \alpha |\epsilon|^{-\alpha-1}, \quad \epsilon \leq -1. \quad (10)$$

Figure 7 shows the mean and standard deviation of ΔE_N against N for $\alpha = 2, 3$, and 4. At sufficiently large N , the two quantities become proportional to each other, indicating a single energy scale $\Delta E_N \sim N^\omega$. The exponent ω can be related to α from the following consideration. On a chain of length N , there are $N(N - 1)/2$ possible pairings. The lowest pairing energy ϵ_{\min} is determined by the condition $N^2 |\epsilon_{\min}|^{-\alpha} \sim 1$. Hence $\epsilon_{\min} \sim -N^{2/\alpha}$. Assuming the energy cost for breaking a chain into two halves is dominated by ϵ_{\min} of the strongest bond, we obtain,

$$\omega = 2/\alpha, \quad (11)$$

which agrees well with the numerical data.

We have also investigated the distribution of the pairing distance under Eq. (10). Interestingly, the results are

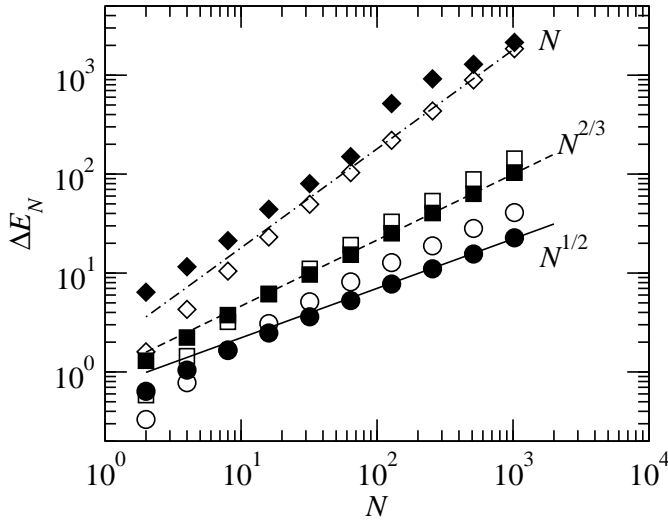


Fig. 7. Power-law distribution of the pairing energies: $\alpha = 2$ (diamond), $\alpha = 3$ (square), and $\alpha = 4$ (circle). Open symbols represent the mean value of ΔE_N while filled symbols represent its standard deviation. Solid, dashed, and dot-dashed lines indicate corresponding power-laws.

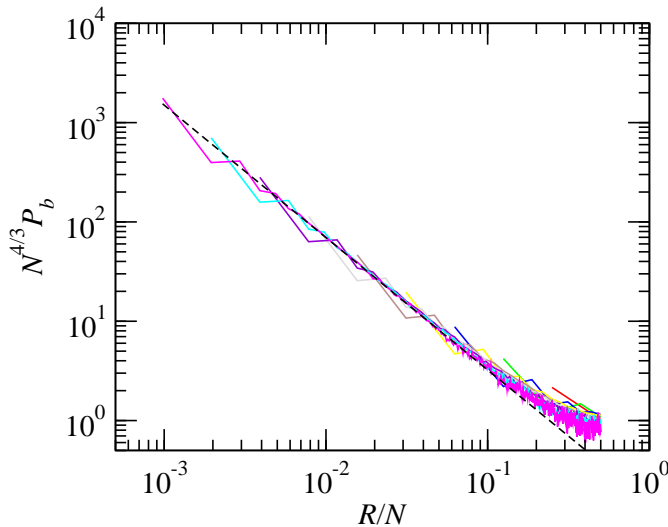


Fig. 8. Scaling plot of the distribution of the optimal break point along a chain of length N for the power-law pairing energy model.

quite insensitive to the value of α , and the exponent η is unchanged from its value $-4/3$ under (2). Figure 8 shows a representative case at $\alpha = 2$. The result is nearly identical to Fig. 4(b). The good data collapse confirms validity of Eq. (7) for power-law pairing energies.

6 Summary and conclusions

In this paper we have investigated properties of the ground state of RNA secondary structure models, and the transition to the molten phase at a finite temperature. We have focused our attention on the excess energy ΔE_N (and the

similarly defined excess free energy ΔF_N) of a chain of N nucleotides due to the presence of boundaries. Since any pairing of two bases automatically splices out a finite segment of the chain, this excess energy defines the characteristic energy scale for the competition between base pairing on a given length scale (measured by the number of nucleotides inbetween) and the adjustments in the secondary structure necessary in order to accommodate the pairing. From numerical investigations of a random energy model with exponential distribution of pairing energies, and a random sequence model with more realistic base pairing and base stacking energies, we have established that ΔF_N has a fluctuation proportional to $\ln N$ in the entire low temperature glass phase. The mean value of ΔF_N , on the other hand, acquires a $\ln^2 N$ term due to accumulation of contributions from smaller scales.

As temperature increases towards the transition, we observe that fluctuations of ΔF_N , or equivalently, variation of the free energy cost to accommodate an inserted pair [i.e., the relative strength of different terms in the sum in Eq. (4)] decreases, hence base pairing becomes less specific. As $T \rightarrow T_g$, the amplitude of the $\ln N$ term vanishes quadratically with the distance to the critical point. This behavior is in striking resemblance to the glass transition of an elastic manifold in two dimensions subject to a random, uncorrelated potential [33,34]. It would be interesting to quantify this connection mathematically.

We have also studied scaling properties in the ground state under a power-law distribution of the pairing energies $\epsilon_{i,j}$. Such distributions may be encountered in a coarse-grained description of real RNA molecules with sequence design[35,36]. In this case, ΔE_N competes with the strongest bond on the chain. Based on extremal statistics arguments, we were able to express the exponent ω characterizing the power-law growth of ΔE_N with N in terms of the exponent α for the power-law distribution of $\epsilon_{i,j}$. This relation is verified by numerical data.

Geometrical properties of base pairing in the RNA secondary structure can be characterized with the distribution of pairing distances. Our studies of the ground state shows that this distribution is well described by a power-law decreasing function with an exponent $\eta = -4/3$, in agreement with previous findings[15]. This behavior is surprisingly insensitive to the models used for the bond energies. In the molten phase, however, it takes the value $\eta_0 = -3/2$. It would be desirable to find an analytic foundation for these observations.

LHT would like to thank Ralf Bundschuh and Terry Hwa for many interesting discussions on the problem. Research is supported in part by the Research Grants Council of the Hong Kong SAR under grant HKBU 2061/01P. Computations were carried out at HKBU's High Performance Cluster Computing Centre Supported by Dell and Intel. We gratefully acknowledge the support of the BIOSUPPORT project (<http://bioinfo.hku.hk>) for providing bioinformatics resources and computational services from the HKU Computer Centre.

Note added: after submission of the paper we became aware of a manuscript by M. Lässig and K. J. Wiese[37]

where a field-theoretic renormalization group treatment of the glass transition is presented. The analysis has been further refined[38] and yielded a value $\zeta_g \simeq 0.64$ at the glass transition.

References

1. B. Alberts, A. Johnson, J. Lewis, M. Raff, K. Roberts, P. Walter, *Molecular Biology of the Cell* (Garland Science, New York, 2002).
2. K.A. Dill, S. Bromberg, K. Yue, K.M. Fiebig, D.P. Yee, P.D. Thomas, H.S. Chan, *Protein Sci.* **4**, 561 (1995).
3. J.N. Onuchic, Z. Luthey-Schulten, P.G. Wolynes, *Annu. Rev. Phys. Chem.* **48**, 545 (1997).
4. E.I. Shakhnovich, *Curr. Opin. Struct. Biol.* **7**, 29 (1997).
5. O. Schueler-Furman, C. Wang, P. Bradley, K. Misura, D. Baker, *Science* **310**, 638 (2005).
6. C.D. Snow, E.J. Sorin, Y.M. Rhee, V.S. Pande, *Annu Rev Biophys Biomol Struct.* **34**, 43 (2005).
7. For a review, see T. Garel, H. Orland, E. Pitard, in *Spin Glasses and Random Fields*, A.P. Young Ed. (World Scientific, 1998), p. 387.
8. T. Hwa, *Nature* **399**, 17 (1999).
9. I. Tinoco, Jr., C. Bustamante, *J. Mol. Biol.* **293**, 271 (1999).
10. *RNA Structure and Function*, Ed. by R.W. Simons, M. Grunberg-Manago (Cold-Spring Harbor 1998).
11. *Nucleic Acids in Chemistry and Biology*, Ed. by G.M. Blackburn, M.J. Gait (IRL Press, Oxford, 1990).
12. M.L.M. Anderson, *Nucleic Acid Hybridization* (Springer, New York, 1998).
13. For a recent review see R. Bundschuh, U. Gerland, *Eur. Phys. J. E* **19**, 319 (2006).
14. M. Zuker, D. Sankoff, *Bull. Math. Biol.* **46**, 591 (1984); M. Zuker, *Science* **244**, 48 (1989).
15. R. Bundschuh, T. Hwa, *Phys. Rev. Lett.* **83**, 1479 (1999); *Phys. Rev. E* **65**, 031903 (2002).
16. R. Nussinov, G. Pieczenik, J.R. Griggs, D.J. Kleitman, *SIAM J. Appl. Math.* **35**, 68 (1978).
17. R. Durbin, S.R. Eddy, A. Krogh, G. Mitchison, *Biological Sequence Analysis* (Cambridge University Press, Cambridge, England, 1998).
18. P.-G. de Gennes, *Biopolymers* **6**, 715 (1968).
19. P.G. Higgs, *Phys. Rev. Lett.* **76**, 704 (1996); *Q. Rev. Biophys.* **33**, 199 (2000).
20. A. Pagnani, G. Parisi, F. Ricci-Tersenghi, *Phys. Rev. Lett.* **84**, 2026 (2000).
21. A.K. Hartmann, *Phys. Rev. Lett.* **86**, 1382 (2001).
22. F. Krzakala, M. Mézard, M. Müller, *Europhys. Lett.* **57**, 752 (2002); M. Müller, F. Krzakala, M. Mézard, *Eur. Phys. J. E* **9**, 67 (2002); M. Müller, *Phys. Rev. E* **67**, 021914 (2003).
23. E. Marinari, A. Pagnani, F. Ricci-Tersenghi, *Phys. Rev. E* **65**, 041919 (2002).
24. M. Mézard, *J. Physique* **51**: 1831 (1990).
25. J. SantaLucia Jr., *Proc. Nat. Acad. Sci. USA* **95**, 1460 (1998).
26. S. Karlin, A. Dembo, *Adv. Appl. Probab.* **24**, 113 (1992).
27. L.-H. Tang, H. Chaté, *Phys. Rev. Lett.* **86**, 830 (2001).
28. Y.-K. Yu, T. Hwa, *J. Comp. Biol.* **8**, 249 (2001).
29. T. Hwa, E. Marinari, K. Sneppen, L.-H. Tang, *Proc. Nat. Acad. Sci.* **100**, 4411 (2003).
30. T. Halpin-Healy, Y.-C. Zhang, *Phys. Rep.* **254**, 215 (1995).
31. J. Krug, P. Meakin, *J. Phys. A* **23**, L987 (1990).
32. L.-H. Tang, B.M. Forrest, D.E. Wolf, *Phys. Rev. A* **45**, 7162 (1992).
33. C. Zeng, P.L. Leath, T. Hwa, *Phys. Rev. Lett.* **83**, 4860 (1999).
34. D. Carpentier, P. Le Doussal, *Phys. Rev. B* **55**, 12128 (1997); and references therein.
35. R. Mukhopadhyay, E. Emberly, C. Tang, N.S. Wingreen, *Phys. Rev. E* **68**, 041904 (2003).
36. F.J. Isaacs, D.J. Dwyer, J.J. Collins, *Nat. Biotechnol.* **24**, 545 (2006).
37. M. Lässig, K. J. Wiese, *Phys. Rev. Lett.* **96**, 228101 (2006).
38. F. David, K. J. Wiese, q-bio.BM/0607044.

